



Sanhuang Jiangtang tablet protects type 2 diabetes osteoporosis via AKT-GSK3 β -NFATc1 signaling pathway by integrating bioinformatics analysis and experimental validation

Qi He^{a,b,1}, Junzheng Yang^{a,b,1}, Gangyu Zhang^{a,b}, Delong Chen^c, Meng Zhang^d, Zhaofeng Pan^{a,b}, Zihao Wang^e, Lijun Su^{a,b}, Jiaxu Zeng^{a,b}, Baohua Wang^{f,***}, Haibin Wang^{g,**}, Peng Chen^{g,*}

^a 1st School of Medicine, Guangzhou University of Chinese Medicine, 12 Jichang Road, Baiyun Area, Guangzhou, 510405, PR China

^b The Laboratory of Orthopaedics and Traumatology of Lingnan Medical Research Center, Guangzhou University of Chinese Medicine, Guangzhou, 510405, PR China

^c Department of Orthopaedic Surgery, Clifford Hospital, Jinan University, Guangzhou, 510006, PR China

^d Department of Orthopedics, Henan Provincial People's Hospital, People's Hospital of Zhengzhou University, People's Hospital of Henan University, Zhengzhou, Henan, 450003, PR China

^e Queen's University Belfast, University Road, Belfast, Northern Ireland, BT7 1NN, United Kingdom

^f Department of Endocrinology, First Affiliated Hospital, Guangzhou University of Chinese Medicine, Guangzhou, 510405, PR China

^g Department of Orthopaedics, First Affiliated Hospital, Guangzhou University of Chinese Medicine, 12 Jichang Road, Baiyun Area, Guangzhou, 510405, PR China

ARTICLE INFO

Keywords:

Sanhuang jiangtang tablet
Type 2 diabetes osteoporosis
Bioinformatics
AKT-GSK3 β -NFATc1 signaling pathway

ABSTRACT

Ethnopharmacological relevance: Sanhuang Jiangtang tablet (SHJTT), has been widely used to treat type 2 diabetes mellitus (T2DM). However, the potential and mechanism of SHJTT in treating type 2 diabetes osteoporosis (T2DOP) has not been reported.

Aim of the study: The aim of this work was to investigate the role and the underlying molecular mechanism of SHJTT in managing type 2 diabetes osteoporosis.

Materials and methods: The target genes of each component consisting of SHJTT were obtained by searching the ETCM database. The target genes of osteoporosis and diabetes were individually acquired by analyzing the DisGeNET and OMIM disease databases. Then the potential therapeutic genes were obtained from the intersection of the herbal medicine targets and the disease targets which were imported into the R and STRING platform for the analysis of GO terms, KEGG pathways and PPI network. The key modules of PPI network were constructed by Cytoscape software. Finally, leptin receptor deficiency (db/db) mice were confirmed as an animal model of type 2 diabetic osteoporosis (T2DOP) through phenotype assessment and the key genes of SHJTT against T2DOP were validated by quantitative real-time PCR (qRT-PCR).

Results: A total of 786 target genes of SHJTT were obtained from ETCM. Simultaneously, a total of 3906 osteoporosis and type 2 diabetes associated targets were acquired from DisGeNET and OMIM databases. Then, 97 common targets were found by overlapping them. On the basis of the GO and KEGG enrichment analysis and PPI network, we found that the related pathway of SHJTT in type 2 diabetes osteoporosis was AKT-GSK3 β -NFATc1 pathway which is tightly associated with osteoclast differentiation. The expression of key genes including *Akt1*, *Mapk3*, *Gsk3 β* , *Mmp9*, *Nfkb1* were significantly down-regulated by SHJTT in T2DOP mice ($p < 0.05$).

Conclusions: SHJTT had a protective effect on T2DOP via regulating AKT-GSK3 β -NFATc1 signaling pathway. This study might provide a theoretical basis for the application of SHJTT for the treatment of type 2 diabetic osteoporosis.

* Corresponding author.

** Corresponding author.

*** Corresponding author.

E-mail addresses: wangbaohua@gzhtcm.edu.cn (B. Wang), hipknee@163.com (H. Wang), docchen777@gmail.com (P. Chen).

¹ These authors contributed equally to this work.

1. Introduction

The morbidity of type 2 diabetes mellitus (T2DM) increases with economic development and extension of life spans, posing a substantial psychological challenge on patients and heavy economic burden on the healthcare system (Khan et al., 2020). Accumulating studies had shown that 1–3 times risk of fractures could occur in T2DM patients indicating that skeletal fragility-related diseases such as osteoporosis should be taken into account as the severe complications associated with T2DM (Janghorbani, Van Dam, Willett and Hu, 2007; Napoli et al., 2017; Shanbhogue, Mitchell, Rosen and Bouxsein, 2016; Strotmeyer et al., 2005). Unfortunately, less attention was attracted to osteoporosis than other diabetic complications such as cardiovascular disease, kidney disease as well as brain disorders (Abdulameer, Sulaiman, Hassali, Subramaniam and Sahib, 2013; Hamann, Kirschner, Günther and Hofbauer, 2012). Therefore, it is urgent to investigate the effective approach to manage type 2 diabetic osteoporosis (T2DOP). The main treatments of T2DOP depend on hypoglycemic drugs combined with anti-osteoporotic drugs (Vestergaard, 2007). T2DOP currently has little monotherapy, thus the exploration of novel targeted therapeutic agents for T2DOP may lead to an opportunity to break through the bottleneck of current clinical treatment status. For millennia, herbal medicines especially Traditional Chinese Medicine had played a significant role in maintaining health. Many studies had demonstrated that TCM is an effective strategy to ameliorate T2DM (Cui et al., 2018; Guo et al., 2019; Tian et al., 2013).

Sanhuang Jiangtang tablet, based on Supplemented Taohe Chengqi decoction, consists of Huangqi (*Radix Astragali*), Dihuang (*Rehmannia glutinosa* (Gaertn.) DC.), Dahuang (*Rheum palmatum* L), Shanyao (*Dioscorea batatas*), Gegen (*Radix Puerariae Lobatae*) and Gancao (*Glycyrrhiza uralensis* Fisch). SHJTT is an effective medicine on diabetes. Although there are a few pharmacological studies on this formula in English-language databases, multiple researches about its herbal ingredients being used in the treatment of diabetes and even osteoporosis (Deng, Xiong and Kuang, 2004; Zhu, Xiong and Lin, 1997). Huangqi is widely used to treat diabetes in China due to the great clinical effect (Nie et al., 2014). Yue et al. revealed that Huangqi may stimulate insulin secretion, improve insulin resistance and promote glucose utilization by systematic analysis (Yue et al., 2017). A systematic review based on clinical and experiment research indicated that Shanyao had both effect on reducing blood glucose and increasing bone mass (Sun et al., 2020). Another review about Gegen showed that it can enhance the glucose-lowering effect meanwhile declining the adverse events (Yang et al., 2019). According to the review written by Liu et al., those formulas contain Dihuang will enhance the effect of anti-osteoporosis (Liu et al., 2017). Taken together, we hypothesized that SHJTT combined with the above herbs could not only treat diabetes, but also have an anti-osteoporosis effect.

In this study, the mechanism of SHJTT therapy for T2DOP was explored through bioinformatics analysis and experimental verification. Due to SHJTT widely used in the clinical treatment of T2DM, we firstly put forward the hypothesis that it may be involved in bone remodeling to treat OP caused by T2DM. Subsequently, the targets of SHJTT against T2DM and OP were obtained. Module analysis was applied to generate the key genes and core signaling pathways. Finally, we conducted in-vivo experiments to verify the therapeutic effects of SHJTT on T2DOP. Our research maybe accounts for the molecular mechanism of underlying SHJTT and provides a theoretical groundwork for extensive use of SHJTT in the treatment of T2DOP.

2. Methods

2.1. Preparation of SHJTT

SHJTT consists of six types of TCM ingredients (Table 1). All SHJTTs (Product Approval Number: Z20070824) were purchased from the First Affiliated Hospital of Guangzhou University of Traditional Chinese

Medicine. All herbs' botanical names listed in Table 1 can be searched in "The Plant List" (www.theplantlist.org) and the indexes of them were congruent with the standards of the Chinese Pharmacopoeia (2010).

2.2. Data preparation

2.2.1. Screening the target genes of the Sanhuang Jiangtang tablet

SHJTT mainly contains six Chinese herbal medicines: Huangqi (*Hedysarum Multijugum Maxim*), Dihuang (*Rehmannia glutinosa Libosch*), Dahuang (*Radix Rhei Et Rhizome*), Shanyao (*Rhizoma Dioscoreae*), Gegen (*Radix Puerariae*) and Gancao (*licorice*). The Encyclopedia of Traditional Chinese Medicine (ETCM), a comprehensive database, was used to obtain the target genes of SHJTT (Xu et al., 2019). The ETCM not only integrates active chemical ingredients, candidate target genes, but also provides systematic analysis of target genes. Further, the target genes from the ETCM were predicted by MedChem Studio (version 3.0) and those genes with high structural similarity (Tanimoto score > 0.8) to active components would be selected.

2.2.2. Acquiring the disease targets of osteoporosis and diabetes

Disease-gene association database (DisGeNET) and Online Mendelian Inheritance in Man (OMIM) were used to screened relative disease targets. We input the disease keywords such as osteoporosis, type 2 diabetes mellitus respectively. Then we combined the results from two databases to improve the accuracy of prediction.

2.2.3. Obtaining the potential therapeutic targets of SHJTT on diabetic osteoporosis

We imported target genes of SHJTT, osteoporosis and type 2 diabetes mellitus into R (version 3.6.3). Then the 'VennDiagram' R package was used to generate a Venn diagram intersected by the above third part. Furthermore, we could obtain the gene interaction network about SHJTT treating osteoporosis and type 2 diabetes mellitus.

2.3. Bioinformatic analysis

2.3.1. Assessing the enrichment analysis of potential genes

'DOSE', 'org.Hs.eg.db', 'clusterProfiler' and 'string' R packages were used to accomplish the enrichment analysis of potential genes screened by intersection. The target genes were read into the R studio and we could obtain the outcomes of Gene Ontology (GO) functional annotations and Kyoto Encyclopedia of Genes and Genomes (KEGG) pathways. Finally, the enrichment analysis of biological process (BP), molecular function (MF) and KEGG were mapped.

2.3.2. Establishment of the PPI network

The potential therapeutic targets were input to the STRING database and revised by high confidence (confidence score ≥ 0.7). Then, the TSV file was imported into Cytoscape software (version 3.7.1) and protein-protein interaction (PPI) network was visualized by the software. Furthermore, MCODE cluster analytical tool was performed to generate the correlated functions network module.

Table 1
The ingredients of Sanhuang Jiangtang tablet.

Chinese name	Botanical names	Origin	Amount in preparation (g)
Huangqi	<i>Astragalus membranaceus</i> (Fisch.) Bunge	Nei meng gu	30
Dihuang	<i>Rehmannia glutinosa</i> (Gaertn.) DC.	Hu bei	15
Dahuang	<i>Rheum palmatum</i> L	Si chuan	6
Gegen	<i>Pueraria lobata</i> (Willd.) Ohwi	Liao ning	15
Shanyao	<i>Dioscorea batatas</i> Decne.	He nan	15
Gancao	<i>Glycyrrhiza uralensis</i> Fisch	Xin jiang	5

2.4. Animal model and experimental intervention

Six-week-old male C57BL/Ks db/db mice with T2DM (30–40 g) and C57BL/6 J mice (20–25 g) were provided by the Animal Laboratory Center of Nanjing university (SCXK (Su) 2018-0008). The genetically diabetic mouse (db/db) has a homozygous point mutation on the chromosome 4 that lacks a functional hypothalamic leptin receptor (H. Chen et al., 1996; Friedman, Leibel, Siegel, Walsh and Bahary, 1991; Yiying Zhang et al., 1994). The syndrome of type 2 diabetes mellitus in db/db mice is alike to type 2 diabetes patients and is characterized by obesity, insulin resistance, hyperinsulinemia and progressive hyperglycemia (Giesbertz et al., 2015; Portha, 2005; Yoon et al., 1988). The mice were maintained on an alternating 12 h light/dark cycle with a temperature of 22–25 °C and humidity of 55–60% in the Laboratory Animal Center of Guangzhou University of Traditional Chinese Medicine (SYXK (Yue) 2018-0034). After adaptively feeding for 1 week, the db/db mice were randomly divided into two groups (n = 10 in each group): model group and SHJTT group. And the C57BL/6 J mice were used as wild-type group (n = 10). Throughout the experiment, mice were given 0.5ml distilled water orally for 8 weeks in wild-type and model groups. The SHJTT group were perfused with SHJTT solution (2.6 g/kg body weight) following the same dose and schedule (Fig. 1). The dosage of mice intragastric administration was calculated according to the dose equivalents between humans and laboratory animals based on ratios of body surface area (Ralph D, 2008). All the experimental steps used in our study were approved by the Ethics Committee of the First Affiliated Hospital of Guangzhou University of Chinese Medicine (License no. TCMF1-2019056).

2.5. Bone densitometry

Model iNSiGHT VET dual-energy X-ray absorptiometry (DXA, Osteosys, Korea) was used to measure the whole Lower limbs bone mineral density (BMD) and bone mineral content (BMC). Mice were anesthetized by intraperitoneal injection of 0.5% chloral hydrate (0.2 ml–0.3 ml). Sedated mice were then placed on the scanning table in a prostrate position. Each DXA measurement took about 25 s, including 10 s of radiation output (Yeu et al., 2019). With the software provided by the manufacturer, the embedded DXA algorithm was used to calculate the body composition value.

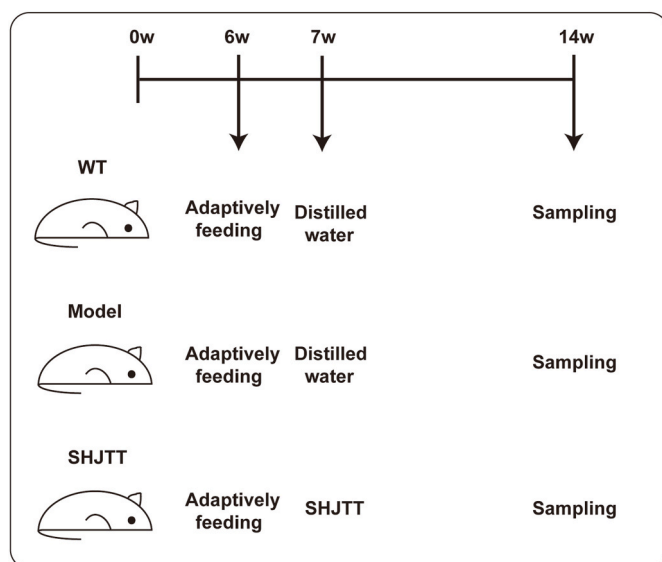


Fig. 1. Schematic diagram of the animal experimental design. w: week; db/db: type 2 diabetic mice with Leptin receptor deficiency; and db/db + SHJTT: db/db mice were perfused with SHJTT solution.

2.6. Micro-CT scanning

All the mice were sacrificed by cervical dislocation, and the left tibiae were isolated and fixed in 4% paraformaldehyde for 24 h. Samples were then washed and stored in phosphate buffered saline until further use. The bones were scanned with a Skyscan 1172 micro-CT scanner (Bruker, Belgium), in rigid plastic tubes containing 70% ethanol. Then, the tibia was analyzed by a micro-CT imaging system with 80 kV voltage, 100 μ A electricity, 0.4° rotation step and 5 μ m slice thickness. After scanning, using Skyscan NRecon software and the Feldkamp-Davis-Kress algorithm, the two-dimensional image sequence is automatically reconstructed into a three-dimensional volume of 15.9 μ m isotropic voxel size. The tibial trabecular microstructure was analyzed by selecting a height of 1.0 mm volume of interest (VOI), starting from 0.45 mm below the proximal tibia growth plate to 1.0 mm at the distal end. And the cortical bone analysis selected a VOI (1 mm) at the upper 5 mm (D. Chen et al., 2020). The structural parameters for evaluating the trabecular bone, including bone volume/tissue volume (BV/TV, %), trabecular thickness (Tb.Th, mm), trabecular separation (Tb.Sp, mm), trabecular number (Tb.N, 1/mm) and structure model index (SMI), while cortical bone thickness (Ct.Th, mm), cortical bone area (Ct.Ar, mm²) were measured to observe the cortical bone parameters. The above data was manipulated and analyzed using the Custom Analysis program (CTAn, Skyscan).

2.7. Bone histomorphometric analysis

14% ethylenediaminetetraacetic acid (EDTA, Sigma-Aldrich) were used to decalcify left tibia at 37 °C for 1 week. Next, all samples were dehydrated by a gradient series of ethanol, and then embedded in paraffin (Zhao et al., 2019). After the paraffin block was trimmed, 5 μ m-thick sections were cut on a paraffin slicing machine and stained with hematoxylin and eosin (Solarbio, Beijing, China) and TRAcP. Sections were imaged with an Olympus BX53 light microscope (Olympus America). Bone histomorphometric parameters, including the osteoblast surface ratio (Ob.S/BS), number of osteoclasts (Ob.N/BS, 1/mm) and osteoclast surface/bone surface (Oc.S/BS) were analyzed by using Image J software (Wayne Rasband, National Institutes of Health, USA).

2.8. Total RNA isolation and quantitative real-time PCR analysis

For total RNA isolation, fresh whole right tibia was snap-frozen in liquid nitrogen and grounded to a fine powder with a mortar and pestle. By using TRIzol Reagent (Invitrogen, Carlsbad, CA, USA), total RNA was extracted and measured quality by Nanodrop 2000 (Thermo Scientific, Rockford, IL, USA). 100ng of total RNA were reverse-transcribed into cDNA through using Evo M-MLV RT Kit (AG, China). QRT-PCR was performed using SYBR Green Pro Tap (AG, China) in a Bio-Rad CFX96 device with the specific primers listed in Table 2. Using the following parameters for PCR amplification: 40 cycles of 95 °C for 30 s, 95 °C for 5 s, and 60 °C for 40 s, and a final extension step of 65 °C 5 s, 0.5 °C

Table 2
Quantitative real-time PCR primer sequences.

Genes	Forward (5'-3')	Reverse (5'-3')
<i>Akt1</i>	GGACTACTTGCACTCCGAGAAG	CATAGTGGCACCCTCTTGATC
<i>Pik3ca</i>	CACCTGAACAGACAAGTAGAGGC	GCAAAGCATCCATGAAGTCTGGC
<i>Nfkb1</i>	CTGACCTGAGCCTTCTGGAC	GCAGGCTATTGCTCATACA
<i>Gsk3β</i>	GAGCCACTGATTACACGTCCAG	CCAACTGATCCACACCACTGTC
<i>Mapk3</i>	GGCTTTCTGACGGAGTATGTGG	GTTGGAGAGCATCTCAGCCAGA
<i>Ctsk</i>	CCAGTGGGAGCTATGGAAGA	AAGTGGTTCATGGCCAGTTC
<i>Acp5</i>	CAGCAGCCAAGGAGGACTAC	ACATAGCCACACCGTTC
<i>Mmp9</i>	CGTGTCTGGAGATTCGACTTGA	TTGGAAACTCACACGCCAGA
<i>Atp6v0d2</i>	GTGAGACCTTGAAGTCTGAA	GAGAAATGTGCTCAGGGGCT
<i>Bglap1</i>	GCAATAAGGTAGTGAACAGACTCC	CCATAGATGCGTTTGTAGCCGG
<i>Runx2</i>	CTTGAACCTCGACCAAGTCTCT	TCATCTGGCTCAGATAGGAGGG
<i>Col1a1</i>	GCTCCTCTTAGGGGCCACT	CCACGTCTCACCATTGGGG
<i>18s</i>	TGGTTGCAAAGCTGAAACTTAAAG	AGTCAAATTAAGCCGCGAGG

increments for 60 s. Relative mRNA expression levels were calculated by using 18s as internal control and the $2^{-\Delta\Delta Ct}$ method. Each sample was assayed at least three times.

2.9. Statistical analysis

All experiments performed were replicated a minimum of three times. Data are expressed as means \pm standard error of mean (SEM). Statistical analysis was by one-way analysis of variance (ANOVA), followed by Turkey's multiple comparison test for multiple groups, and comparison between two groups was detected using student's t-test (GraphPad Prism 7.0). Differences were considered statistically significant ($P < 0.05$).

3. Results

3.1. The target genes of Sanhuang Jiangtang tablet

After inputting the main herbs of SHJTT, we obtained prediction genes from ETCM database. Through eliminating the repeated genes, we totally screened 786 target genes.

3.2. The therapeutic genes of SHJTT in osteoporosis and diabetes

Through searching the target genes of osteoporosis and diabetes in the DisGeNET and OMIM databases, combining the target genes from

both database and deleting the duplicate results, we acquired 1101 disease targets for osteoporosis and 2805 for diabetes. Then, the intersection of target genes of SHJTT, osteoporosis and diabetes were mapped (Fig. 2A). The Venn diagram revealed that 97 predicted therapeutic targets of SHJTT in osteoporosis and diabetes.

3.3. GO and KEGG pathway analysis of common therapeutic genes

The 97 overlapped genes above were mapped for an enrichment analysis of the GO terms and KEGG pathways (Fig. 2B-E). GO biological process analysis showed that multicellular organismal homeostasis, response to peptide hormone, regulation of small molecule metabolic process, response to steroid hormone, steroid metabolic process, etc. play significant roles in the treatment of SHJTT in osteoporosis and diabetes. GO molecular function analysis revealed that steroid binding, coenzyme binding, nuclear receptor activity, transcription factor activity and direct ligand regulated sequence-specific DNA binding account for the main position of the molecular function of SHJTT in the treatment of osteoporosis and diabetes. The outcome of KEGG pathway analysis unveiled that HIF-1 signaling pathway, insulin resistance, osteoclast differentiation, estrogen signaling pathway and TNF signaling pathway play important roles in related signaling pathways of SHJTT treating in osteoporosis and diabetes.

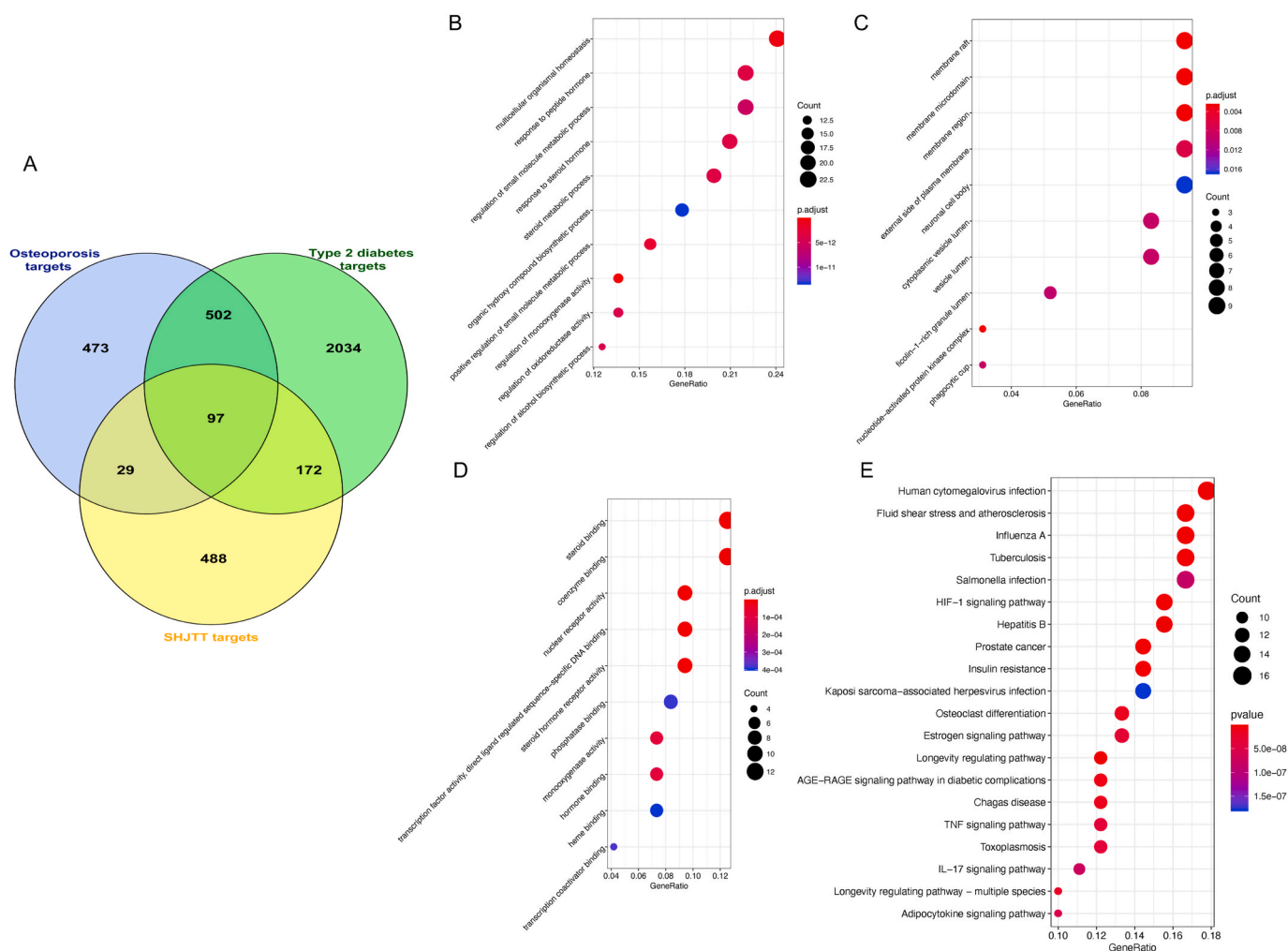


Fig. 2. Venn diagram of drug-disease intersection target of SHJTT for osteoporosis and diabetes (A), Dot plot of the GO biological processes (B), cellular components (C), molecular function (D) and KEGG pathways (E) of common targets of SHJTT in the treatment of osteoporosis and diabetes.

3.4. PPI network of shared genes

The interactions of 97 shared targets were visualized by the PPI network diagram so that we could better understand the potential mechanism of SHJTT in the treatment of osteoporosis and diabetes (Fig. 3A). The network contains 83 nodes and 616 edges. Furthermore, algorithm of MCODE was used to obtain the key modules. On the basis of the network score, the top 3 clusters were obtained (Fig. 3B). 19 hub genes were divided from the whole target genes. It indicates that the hub genes may be key genes in the therapeutic mechanisms which remain to be elucidated.

3.5. SHJTT treatment ameliorated bone microarchitecture in db/db-induced osteoporosis mice

DXA analyses of the whole lower limbs bone indicated that model group has a significantly lower BMD and BMC as compared to wild-type group (Fig. 4B). In the SHJTT group, BMD was higher than model group, and we found no significant difference in BMC. Reconstructed 3D images of the proximal tibia revealed that db/db mice induced significant bone loss and the treatment with SHJTT inhibited bone loss in the db/db mice (Fig. 4A). In the quantitative analysis, BV/TV, Tb.Th, Tb.N were found to be prominently lessened while Tb.Sp, SMI were increased in model group relative to wild-type group (Fig. 4C). Trabecular separation, a parameter inversely proportional to structural connectivity, was increased, suggesting that the trabecular structure was more disjointed

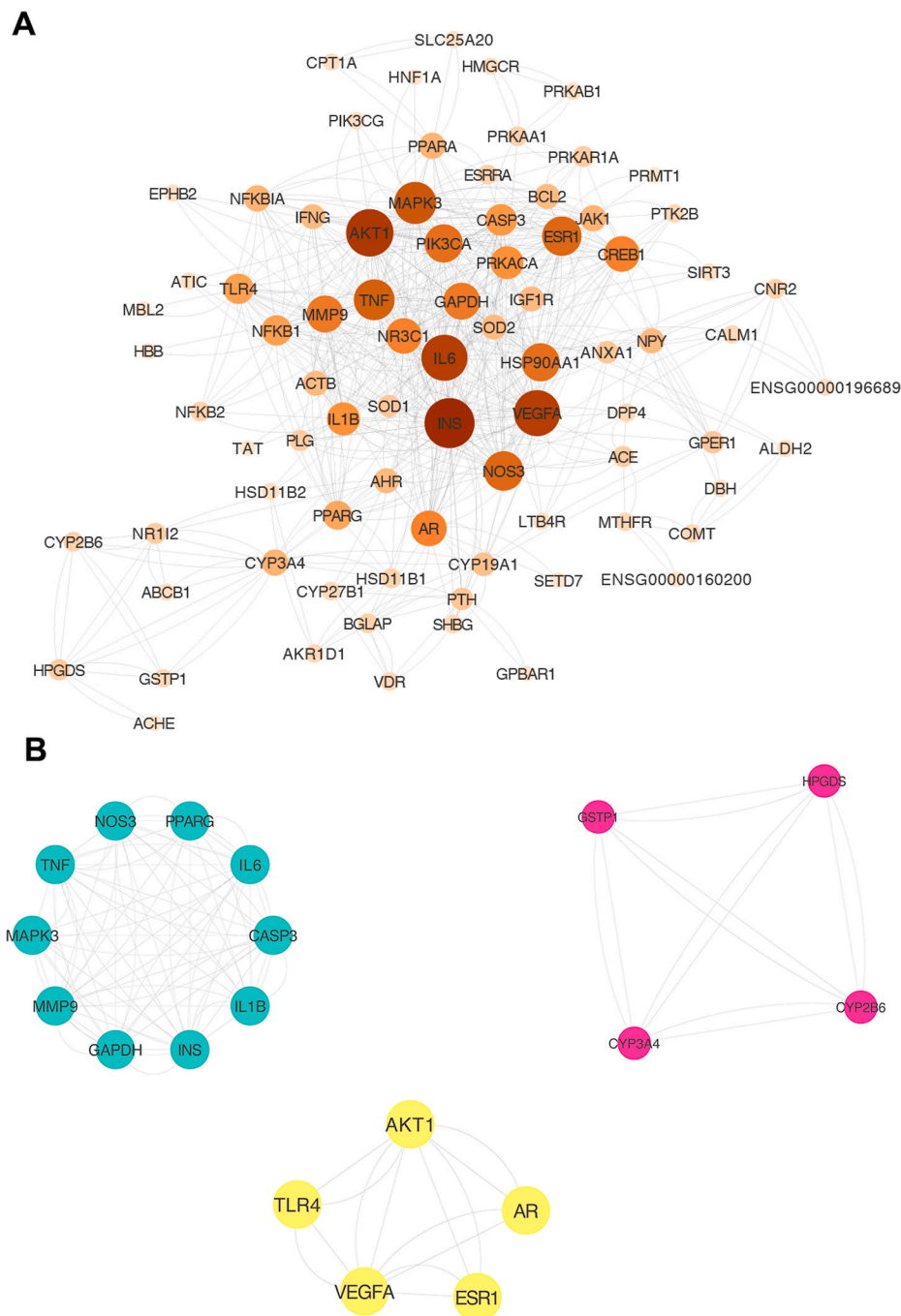


Fig. 3. PPI network diagram (A) of common targets and key module (B) of SHJTT in the treatment of osteoporosis and diabetes.

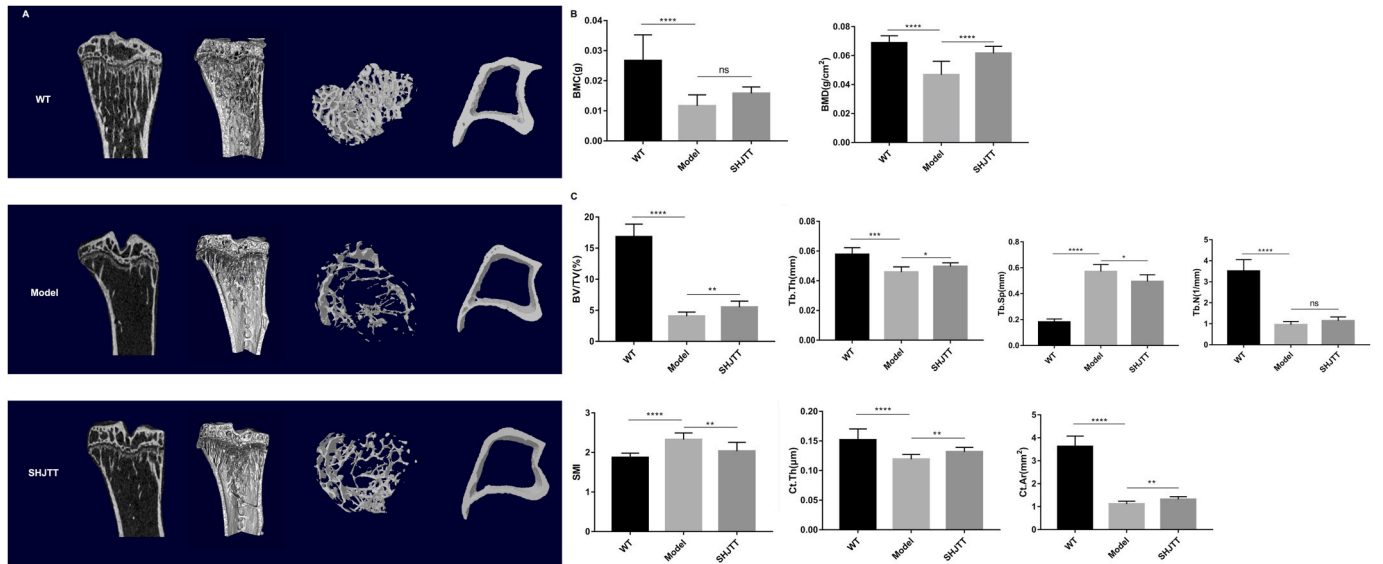


Fig. 4. SHJTT prevents bone loss of murine db/db-induced osteoporosis with T2DM in vivo. (A) Representative 2D and 3D reconstruction micro-CT images of tibiae in the different groups; (B) BMD and BMC were calculated based on DXA results (n = 10); (C) BV/TV, Tb.N, Tb.Sp, Tb.Th, SMI and Ct.Th, Ct.Ar were analyzed based on micro-CT and DXA results (n = 10). All data are expressed as means ± SEM. *P<0.05, **P<0.01, ***P<0.001, ****P<0.0001 (one-way ANOVA with Tukey's multiple comparison test); ns: not significant.

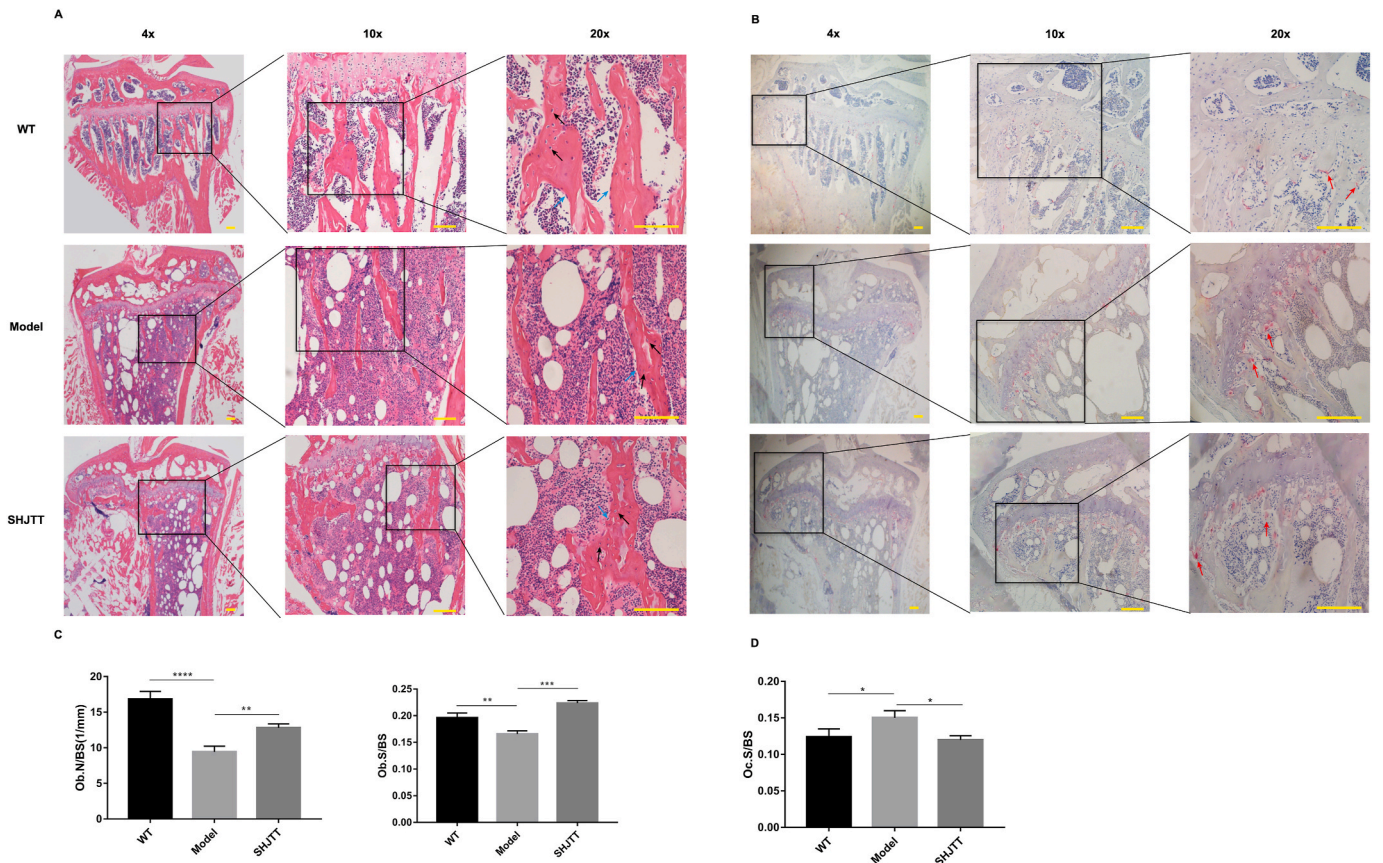


Fig. 5. SHJTT attenuated histomorphological damage of murine db/db-induced osteoporosis with T2DM. Representative H&E and TRACP staining images of proximal tibia (A, B) (Black arrow indicates osteocytes, blue arrow indicates osteoblasts and red arrow indicates osteoblasts; Scale bars = 50 μm). The quantifications of Ob.S/BS, Ob.N/BS, and Oc.S/BS were calculated based on H&E and TRACP staining by using the Image J software (C, D). Data are expressed as means ± SEM. *P<0.05, **P<0.01, ***P<0.001, ****P<0.0001 (one-way ANOVA with Tukey's multiple comparison test); ns: not significant. (For interpretation of the references to colour in this figure legend, the reader is referred to the Web version of this article.)

in db/db mice. This coincided with the increased SMI, which suggests that the normally platelike trabeculae observed in the wild-type mice had been converted to more rodlike structures (Hildebrand and Rüegg-segger, 1997). And the SHJTT treatment group generated a skeletal-protecting phenotype in db/db mice with T2DM, as evidenced by increasing in BV/TV, Tb.Th, Tb.N and decreasing in Tb.Sp, SMI compared with the model group. The model group showed reductions in Ct.Ar and Ct.Th compared with the wild-type group (Fig. 4C). Conversely, we found that the metrics above increased in the SHJTT group.

3.6. SHJTT attenuated bone tissue morphological damage of T2DM-induced osteoporosis in db/db mice

H&E and TRAcP staining of the proximal tibia uncovered thinner, smaller trabeculae with more microcracks in the model group relative to wild-type groups (Fig. 5A, B). In contrast, the SHJTT group showed thickened, coarse trabeculae compared to the model group. Relative to wild-type groups, the Ob.S/BS and Ob.N/BS were consistently reduced in the model group (Fig. 5C). As before, SHJTT markedly decreased the values of Oc.S/BS (Fig. 5D). Altogether, these results significantly suggested that SHJTT was able to hold back histomorphological damage in db/db-induced osteoporosis mice.

3.7. SHJTT facilitates bone formation-related genes expression and reduces the expression of bone resorption-related gene through impairing AKT-GSK3 β -NFATc1 signaling pathway

Gene expression analysis was conducted after crushing all murine right tibia in a mortar with liquid nitrogen. *Runx2*, *Bglap* and *Col1a1* were significantly down-regulated in the model group (Fig. 6F-H). Conversely, the osteoclast-specific genes have been shown to upregulate expression in model group, including *Nfatc1*, *Acp5*, *Mmp9*, *Atp6v0d2* and *Nfkb1* (Fig. 6A-E). *Akt* as a hub gene that obtained from network analysis has association with osteoclasts. The AKT-GSK3 β is one such pathway regulating the expression of *Nfatc1* in osteoclasts (Xiao et al., 2020). Over-expression of *Akt* promoted the phosphorylation of GSK3 β and nuclear localization of NFATc1, and that overexpression of a constitutively active form of GSK3 β attenuates osteoclast formation through downregulation of NFATc1 (Lin et al., 2019; Wu et al., 2017). We identified that the expression of *Akt* and *Nfatc1* in SHJTT group was noticeably lower than model group, while GSK3 β was upregulated (Fig. 6J-L). The decreased gene expression of NFATc1 is consistent with inhibiting osteoclast formation, whereas lower expressions of *Acp5*, *Mmp9* and *Atp6v0d2* correspond well with reduced bone resorptive function. Therefore, the SHJTT leads to promoting bone formation and impaired the efficiency of RANKL-induced osteoclast formation by inhibiting of the Akt-GSK3 β -NFATc1 signaling axis ultimately (Fig. 7).

4. Discussion

Osteoporosis is the most frequent complication from type 2 diabetes, and it is also the main reason for the long-term pain and dysfunction of physical skeleton of diabetic patients (Lecka-Czernik, 2017). The pathogenesis of T2DOP is complex, with many influencing factors, involving the interaction of multiple pathways and the therapeutic options of T2DOP are still largely limited (H. L. Chen, Deng and Li, 2013). It is reported that SHJTT had a good clinical effect on treating T2DM (Xiong, Lin and Zhu, 1997), but none researches have proved that SHJTT can reduce the occurrence of OP induced by T2DM and illuminate the mechanism of SHJTT against T2DOP at the level of molecular at present. On the basis of bioinformatics analysis and experimental verification, we found that AKT-GSK3 β -NFATc1 signaling pathway were mainly involved in the treatment of SHJTT against T2DOP.

According to the enrichment analysis, we found that the SHJTT likely affects osteoclasts through the metabolic pathways. The results of

biological process unveiled that various metabolic processes such as steroid metabolic process, regulation of small molecule metabolic process, etc. be influenced. Besides, the outcomes of KEGG pathways revealed that potential therapeutic targets enriched in osteoclast differentiation, HIF-1 signaling pathway and insulin resistance. Furthermore, the PPI network and key module showed hub genes like *Ins*, *Akt1*, *Mapk3*, *Vegfa*, *Mmp9*, *Nfkb1* and *Esr1* which had great association with bone remodeling and metabolic regulation played significant roles in the mechanism of SHJTT treating in T2DOP. Then, we performed a series of experiments to verify our prediction and analysis.

In this experiment, we firstly used db/db mice as a model of T2DOP. Although the bone phenotype caused by db/db mice remains controversial (Ducy et al., 2000), a large number of researches have testified that serious deterioration in bone microstructure and reduction in bone strength can be observed in type 2 diabetic mice. For example, Ealey KN, He H and others found that bone mass, the mechanical strength and bone formation rate were consistently lower in db/db mice than WT mice (Ealey, Fonseca, Archer and Ward, 2006; He et al., 2004). Besides, Williams et al. further proved that the microstructure of the cancellous and cortical bone of tibia of db/db mice was damaged and the thickness was reduced in cortical bone of vertebrae by micro-CT (Williams et al., 2011). Moreover, the bone formation rate also decreased significantly. Through high-resolution micro-CT and histomorphometric analysis, we further confirmed that the tibia of db/db mice was significantly decreased in bone volume fraction, trabecular thickness and cortical bone thickness. Even bone microstructure was destroyed, which was consistent with the findings of Da Jing et al. (Jing et al., 2016)

SHJTT is a Chinese medicine prescription used to treat T2DM and many other illnesses (Y. Zhang et al., 2016; Zhou et al., 2020). In addition to playing an important role in regulating insulin resistance, hemorheology and microcirculation, SHJTT have different degrees of effects in preventing heart failure and hypertension (Deng et al., 2004; Lebedev, Lyasnikova, Vasilyeva, Babenko and Shlyakhto, 2020; Li, Xiong and Lin, 2000; Miura et al., 2020). By using the murine model of db/db induced type 2 diabetic osteoporosis, SHJTT was demonstrated by histomorphological assessment that it could ameliorate change of bone microarchitecture in such a model. What is more, the quantified parameters from bone histomorphological uncovered that SHJTT increased the number and surface area of osteoblasts and inhibited the increases in the number and area of osteoclasts.

To further clarify the molecular mechanisms underlying the role of SHJTT on bone loss of T2DM, the mRNA expression levels of several genes related to bone metabolism in tibiae were analyzed. RUNX2, BGLAP, ALP and COL1A1 are defined broadly as positive regulator of osteogenic differentiation and bone formation (Drissi et al., 2000; Komori, 2017), whereas NFATc1 serves as a key regulatory factor of osteoclastogenesis (Kobayashi et al., 2001; Nakahama, 2010). In our research, compared with the model group, *Runx2*, *Bglap* and *Col1a1* were upregulated, whereas *Nfatc1*, *Acp5*, *Mmp9*, *Atp6v0d2* and *Nfkb1* were downregulated in SHJTT group. It means that SHJTT can promote osteogenesis and inhibit bone resorption simultaneously (Kanzaki et al., 2016; Walsh et al., 2006).

AKT-GSK3 β -NFATc1 axis, a key signaling pathway in the regulation of osteoclast function, can be stimulated by RANKL-induced signaling pathways in space and time (Z. H. Lee et al., 2002; Moon et al., 2012; Sugatani and Hruska, 2005). Besides, AKT-GSK3 β pathway is closely related to glucose metabolism, which indicates that SHJTT may correct glucose metabolism disorder by AKT-GSK3 β pathway (Huang, Liu, Guo and Su, 2018; J. Lee, Noh, Lim and Kim, 2021). Our results demonstrated that SHJTT down-regulated *Akt1* expression, which abundantly expressed in osteoclasts (Kawamura et al., 2007). Decreasing in AKT contributed to keep the activation of GSK3 β , which reduced downstream NFATc1 transcription to the nucleus, directly suppressing osteoclast differentiation. Thus, these indicated the inhibitory action of SHJTT on the AKT-GSK3 β -NFATc1 pathway in vitro.

Although we showed the protective effect of SHJTT on T2DOP mice

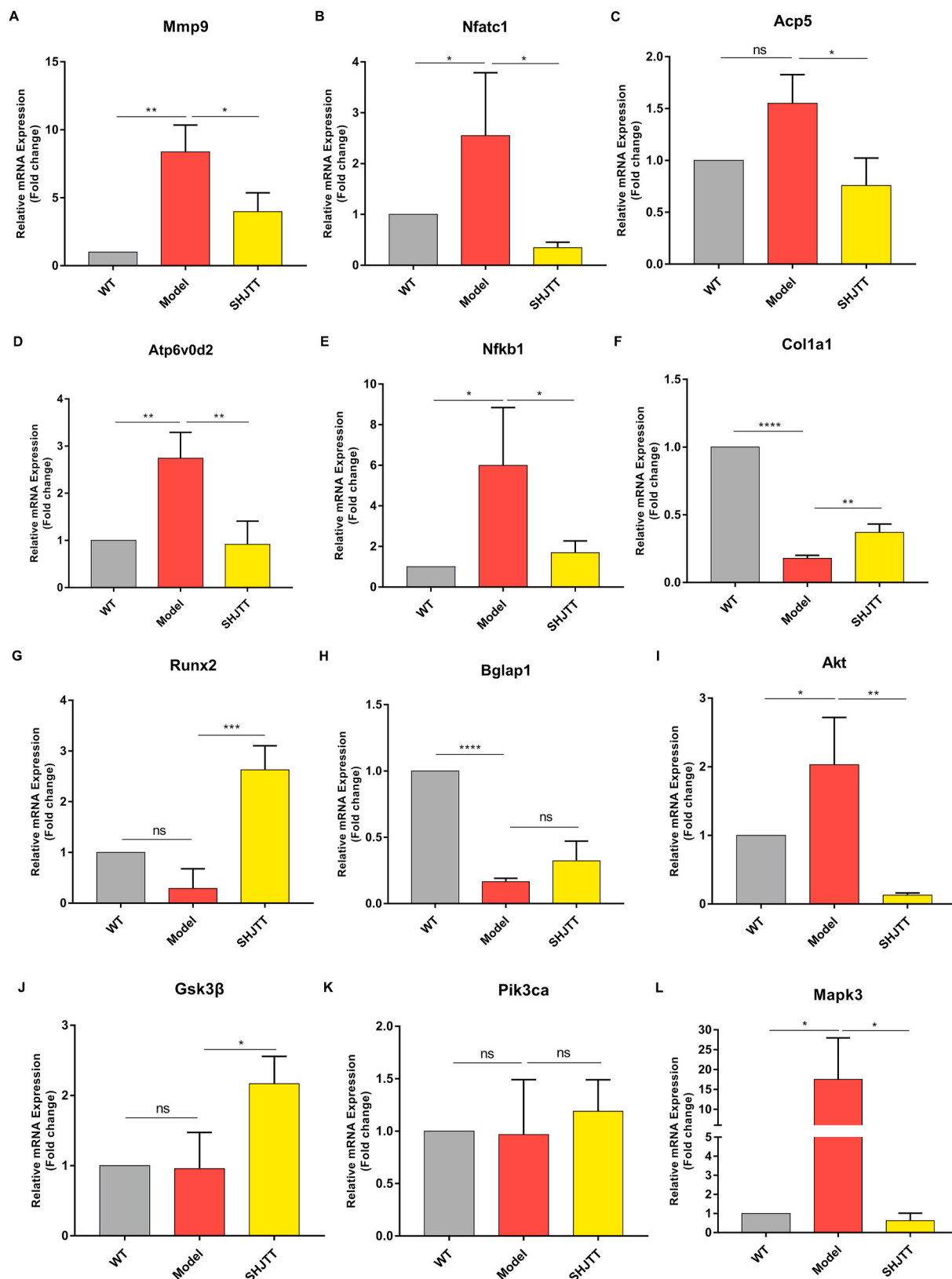


Fig. 6. The effects of SHJTT treatment on the mRNA expression of osteoclastogenesis-specific genes *Nfatc1*, *Acp5*, *Mmp9*, *Atp6v0d2* and *Nfkb1* (A–E), osteogenesis-specific genes *Runx2*, *Bglap1* and *Col1a1* (F–H) and *Akt*, *Gsk3β*, *Mapk3*, *Pik3ca* (J–L). These gene expression levels were standardized to 18s expression. Data are expressed as means ± SEM. * $P < 0.05$, ** $P < 0.01$, *** $P < 0.001$, **** $P < 0.0001$ (one-way ANOVA with Tukey’s multiple comparison test); ns: not significant.

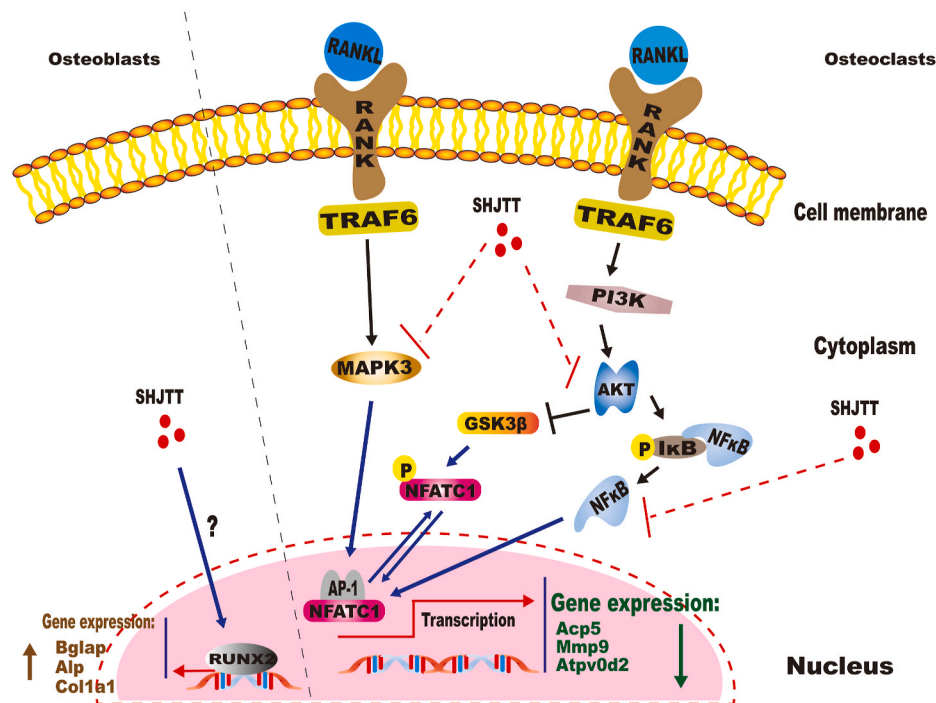


Fig. 7. Schematic diagram of SHJTT function in the differentiation of osteoclast and osteoblast. SHJTT decreased NFATc1 expression to inhibit osteoclast differentiation via suppressing RANKL-induced AKT-GSK3 β , NF- κ B and MAPK signaling activation. Besides, SHJTT upregulated Runx2 expression to promote osteoblast differentiation. '?': undefined.

and also gained insights into its regulating mechanism, this research had a number of limitations and still need further study. First, there was a lack of accurate quantitative index for evaluating T2DM induced osteoporosis with db/db model, and we did not use blood samples to evaluate bone turnover markers and endogenous hormone levels, so we were unable to observe fundamental changes in the balance of bone metabolism in animal models. Second, it was very hard to measure the femoral neck in mice, so we scanned the proximal tibia instead of femoral neck with micro-CT, thus it might not be applicable to patients with type 2 diabetes whose fracture site was in the femur (Shan et al., 2011). Third, we cannot rule out whether the effect of SHJTT on glucose metabolism also plays an anti-osteoporosis role because T2DOP has many causes and we lack cellular experiments and clinical trials to further support this ultimateness (Montagnani, Gonnelli, Alessandri and Nuti, 2011). To sum up, further experiments are required to validate the conclusions of this study and determine its clinical utility.

5. Conclusion

Our research indicates that SHJTT possesses significant anti-osteoporosis activities against db/db-induced type 2 diabetes mellitus mice, which can be attributed to its role in the direct regulation of osteoblast and osteoclast, or through affecting glucose metabolism to regulate bone homeostasis indirectly. Further mechanism revealed that SHJTT has a latent protective effect on T2DOP via regulating AKT-GSK3 β -NFATc1 signaling pathway. In a word, the results of this study suggest that SHJTT could be used as a potential drug for the treatment of T2DOP and further experiments are required to validate the conclusions of this study and determine its clinical utility.

Authors' contributions

Haibin Wang, Peng Chen, and Qi He designed the study. Qi He and Junzheng Yang wrote the manuscript. Baohua Wang, Meng Zhang, Qi He and Junzheng Yang designed the animal experiment. Qi He, Junzheng Yang and Zhaofeng Pan participated in animal experiment. Gangyu

Zhang, Zhaofeng Pan, Qi He and Junzheng Yang analyzed micro-CT data. Qi He and Junzheng Yang performed histological examination. Qi He, Junzheng Yang, Zhaofeng Pan and Jiaxu Zeng participated in qPCR and western blotting. Qi He and Lijun Su performed the statistical analysis. Peng Chen, Qi He, Junzheng Yang and Zihao Wang revised the manuscript.

Data accessibility

The data supporting this study is open access and can be found in the corresponding databases described in this paper.

Declaration of competing interest

All the authors state that they have no interest conflicts for this work.

Acknowledgments

This research was supported by National Natural Science Foundation of China (No. 81774339; NO. 82074462), Major research project of Guangzhou University of Chinese Medicine (No. XK2019012), the Guangdong Science Province and Technology Program project (No. 2017A020213030) and the Guangzhou Science and Technology Planning Project (No. 201707010319).

Abbreviations (alphabetical)

BP	Biological process
BV/TV	Bone volume/tissue volume
Ct.Ar	Cortical bone area
Ct.Th	Cortical bone thickness
DisGeNET	Disease-gene association database
EDTA	Ethylenediaminetetraacetic acid
ETCM	The Encyclopedia of Traditional Chinese Medicine
GO	Gene Ontology
H&E	Hematoxylin and eosin staining

KEGG	Kyoto Encyclopedia of Genes and Genomes
MF	Molecular function
N.Oc/BS	Osteoclast number/bone surface
Ob.N/BS	Number of osteoclasts
Ob.S/BS	Osteoblast surface ratio
Oc.S/BS	Osteoclast surface/bone surface
OMIM	Online Mendelian Inheritance in Man
qRT-PCR	Quantitative real-time PCR
SHJTT	Sanhuang Jiangtang tablet
SMI	Structure model index
T2DOP	Type 2 diabetic osteoporosis
T2DM	Type 2 diabetes mellitus
Tb.Th	Trabecular thickness
Tb.Sp	Trabecular separation
Tb.N	Trabecular number
TCM	Traditional Chinese Medicine
TRAcP	Tartrate resistant acid phosphatase
VOI	The volume of interest

References

- Abdulameer, S.A., Sulaiman, S.S., Hassali, M., Subramaniam, K., Sahib, M., 2013. Psychometric properties and osteoprotective behaviors among type 2 diabetic patients: osteoporosis self-efficacy scale Malay version (OSSES-M). *Osteoporos. Int.* 24 (3), 929–940.
- Chen, D., Ye, Z., Wang, C., Wang, Q., Wang, H., Kuek, V., Xu, J., 2020. Arctiin abrogates osteoclastogenesis and bone resorption via suppressing RANKL-induced ROS and NFATc1 activation. *Pharmacol. Res.* 159, 104944. <https://doi.org/10.1016/j.phrs.2020.104944>.
- Chen, H., Charlat, O., Tartaglia, L., Woolf, E., Weng, X., Ellis, S., Morgenstern, J., 1996. Evidence that the diabetes gene encodes the leptin receptor: identification of a mutation in the leptin receptor gene in db/db mice. *Cell* 84 (3), 491–495. [https://doi.org/10.1016/S0092-8674\(00\)81294-5](https://doi.org/10.1016/S0092-8674(00)81294-5).
- Chen, H.L., Deng, L.L., Li, J.F., 2013. Prevalence of osteoporosis and its associated factors among older men with type 2 diabetes. *Internet J. Endocrinol.* 2013, 285729. <https://doi.org/10.1155/2013/285729>.
- Cui, X., Qian, D.W., Jiang, S., Shang, E.X., Zhu, Z.H., Duan, J.A., 2018. Scutellariae radix and coptidis rhizoma improve glucose and lipid metabolism in T2DM rats via regulation of the metabolic profiling and MAPK/PI3K/Akt signaling pathway. *Int. J. Mol. Sci.* 19 (11) <https://doi.org/10.3390/ijms19113634>.
- Deng, C.Q., Xiong, M.Q., Kuang, X.Y., 2004. [Effect of sanhuang jiangtang recipe on renin-angiotensin system in local myocardium in diabetic rats]. *Zhongguo Zhong Xi Yi Jie He Za Zhi* 24 (4), 348–352.
- Drissi, H., Luc, Q., Shakoori, R., Chuva De Sousa Lopes, S., Choi, J.Y., Terry, A., Stein, G. S., 2000. Transcriptional autoregulation of the bone related Cbfa1/RUNX2 gene. *J. Cell. Physiol.* 184 (3), 341–350. [https://doi.org/10.1002/1097-4652\(200009\)184:3<341::Aid-jcp8>3.0.Co;2-z](https://doi.org/10.1002/1097-4652(200009)184:3<341::Aid-jcp8>3.0.Co;2-z).
- Ducy, P., Amling, M., Takeda, S., Priemel, M., Schilling, A.F., Beil, F.T., Karsenty, G., 2000. Leptin inhibits bone formation through a hypothalamic relay: a central control of bone mass. *Cell* 100 (2), 197–207. [https://doi.org/10.1016/S0092-8674\(00\)81558-5](https://doi.org/10.1016/S0092-8674(00)81558-5).
- Ealey, K.N., Fonseca, D., Archer, M.C., Ward, W.E., 2006. Bone abnormalities in adolescent leptin-deficient mice. *Regul. Pept.* 136 (1–3), 9–13. <https://doi.org/10.1016/j.regpep.2006.04.013>.
- Friedman, J.M., Leibel, R.L., Siegel, D.S., Walsh, J., Bahary, N., 1991. Molecular mapping of the mouse ob mutation. *Genomics* 11 (4), 1054–1062. [https://doi.org/10.1016/0888-7543\(91\)90032-a](https://doi.org/10.1016/0888-7543(91)90032-a).
- Giesbertz, P., Padberg, I., Rein, D., Ecker, J., Höfle, A., Spanier, B., Daniel, H., 2015. Metabolite profiling in plasma and tissues of ob/ob and db/db mice identifies novel markers of obesity and type 2 diabetes. *Diabetologia* 58 (9), 2133–2143. <https://doi.org/10.1007/s00125-015-3656-y>.
- Guo, Q., Niu, W., Li, X., Guo, H., Zhang, N., Wang, X., Wu, L., 2019. Study on hypoglycemic effect of the drug pair of Astragalus radix and Dioscoreae rhizoma in T2DM rats by network pharmacology and metabolomics. *Molecules* 24 (22). <https://doi.org/10.3390/molecules24224050>.
- Hamann, C., Kirschner, S., Günther, K.-P., Hofbauer, L.C., 2012. Bone, sweet bone—osteoporotic fractures in diabetes mellitus. *Nat. Rev. Endocrinol.* 8 (5), 297–305.
- He, H., Liu, R., Desta, T., Leone, C., Gerstenfeld, L.C., Graves, D.T., 2004. Diabetes causes decreased osteoclastogenesis, reduced bone formation, and enhanced apoptosis of osteoblastic cells in bacteria stimulated bone loss. *Endocrinology* 145 (1), 447–452. <https://doi.org/10.1210/en.2003-1239>.
- Hildebrand, T., Rügsegger, P., 1997. A new method for the model-independent assessment of thickness in three-dimensional images. *J. Microsc.* 185 (1), 67–75. <https://doi.org/10.1046/j.1365-2818.1997.1340694.x>.
- Huang, X., Liu, G., Guo, J., Su, Z., 2018. The PI3K/AKT pathway in obesity and type 2 diabetes. *Int. J. Biol. Sci.* 14 (11), 1483–1496. <https://doi.org/10.7150/ijbs.27173>.
- Janghorbani, M., Van Dam, R.M., Willett, W.C., Hu, F.B., 2007. Systematic review of type 1 and type 2 diabetes mellitus and risk of fracture. *Am. J. Epidemiol.* 166 (5), 495–505.
- Jing, D., Luo, E., Cai, J., Tong, S., Zhai, M., Shen, G., Luo, Z., 2016. Mechanical vibration mitigates the decrease of bone quantity and bone quality of leptin receptor-deficient Db/Db mice by promoting bone formation and inhibiting bone resorption. *J. Bone Miner. Res.* 31 (9), 1713–1724. <https://doi.org/10.1002/jbmr.2837>.
- Kanzaki, H., Shinohara, F., Kanako, I., Yamaguchi, Y., Fukaya, S., Miyamoto, Y., Nakamura, Y., 2016. Molecular regulatory mechanisms of osteoclastogenesis through cytoprotective enzymes. *Redox Biol.* 8, 186–191. <https://doi.org/10.1016/j.redox.2016.01.006>.
- Kawamura, N., Kugimiya, F., Oshima, Y., Ohba, S., Ikeda, T., Saito, T., Kawaguchi, H., 2007. Akt1 in osteoblasts and osteoclasts controls bone remodeling. *PLoS One* 2 (10), e1058. <https://doi.org/10.1371/journal.pone.0001058>.
- Khan, M.A.B., Hashim, M.J., King, J.K., Govender, R.D., Mustafa, H., Al Kaabi, J., 2020. Epidemiology of type 2 diabetes—global burden of disease and forecasted trends. *Journal of epidemiology and global health* 10 (1), 107.
- Kobayashi, N., Kadono, Y., Naito, A., Matsumoto, K., Yamamoto, T., Tanaka, S., Inoue, J., 2001. Segregation of TRAF6-mediated signaling pathways clarifies its role in osteoclastogenesis. *EMBO J.* 20 (6), 1271–1280. <https://doi.org/10.1093/emboj/20.6.1271>.
- Komori, T., 2017. Roles of Runx2 in skeletal development. *Adv. Exp. Med. Biol.* 962, 83–93. https://doi.org/10.1007/978-981-10-3233-2_6.
- Lebedev, D.A., Lyasnikova, E.A., Vasilyeva, E.Y., Babenko, A.Y., Shlyakhto, E.V., 2020. Type 2 diabetes mellitus and chronic heart failure with midrange and preserved ejection fraction: a focus on serum biomarkers of fibrosis. *J. Diabetes Res* 2020, 6976153. <https://doi.org/10.1155/2020/6976153>.
- Lecka-Czernik, B., 2017. Diabetes, bone and glucose-lowering agents: basic biology. *Diabetologia* 60 (7), 1163–1169. <https://doi.org/10.1007/s00125-017-4269-4>.
- Lee, J., Noh, S., Lim, S., Kim, B., 2021. Plant extracts for type 2 diabetes: from traditional medicine to modern drug discovery. *Antioxidants* 10 (1). <https://doi.org/10.3390/antiox10010081>.
- Lee, Z.H., Lee, S.E., Kim, C.W., Lee, S.H., Kim, S.W., Kwack, K., Kim, H.H., 2002. IL-1 α stimulation of osteoclast survival through the PI 3-kinase/Akt and ERK pathways. *J. Biochem.* 131 (1), 161–166. <https://doi.org/10.1093/oxfordjournals.jbchem.a003071>.
- Li, S., Xiong, M., Lin, A., 2000. [Contrast observation on preventive effect of different traditional Chinese medicine treatments on coronary artery ligation induced myocardial ischemia in rats with diabetes mellitus]. *Zhongguo Zhong Xi Yi Jie He Za Zhi* 20 (6), 438–440.
- Lin, X., Xiao, Y., Chen, Z., Ma, J., Qiu, W., Zhang, K., Qian, A., 2019. Microtubule actin crosslinking factor 1 (MACF1) knockdown inhibits RANKL-induced osteoclastogenesis via Akt/GSK3 β /NFATc1 signalling pathway. *Mol. Cell. Endocrinol.* 494, 110494. <https://doi.org/10.1016/j.mce.2019.110494>.
- Liu, C., Ma, R., Wang, L., Zhu, R., Liu, H., Guo, Y., Gao, S., 2017. Rehmanniae Radix in osteoporosis: a review of traditional Chinese medicinal uses, phytochemistry, pharmacokinetics and pharmacology. *J. Ethnopharmacol.* 198, 351–362. <https://doi.org/10.1016/j.jep.2017.01.021>.
- Miura, M., Hasegawa, T., Matsumoto, A., Nishiyama, M., Someya, Y., Satoh, W., Sato, H., 2020. Effect of transient elevation of glucose on contractile properties in non-diabetic rat cardiac muscle. *Heart Ves.* <https://doi.org/10.1007/s00380-020-01726-6>.
- Montagnani, A., Gonnelli, S., Alessandri, M., Nuti, R., 2011. Osteoporosis and risk of fracture in patients with diabetes: an update. *Aging Clin. Exp. Res.* 23 (2), 84–90. <https://doi.org/10.1007/bf03351073>.
- Moon, J.B., Kim, J.H., Kim, K., Youn, B.U., Ko, A., Lee, S.Y., Kim, N., 2012. Akt induces osteoclast differentiation through regulating the GSK3 β /NFATc1 signaling cascade. *J. Immunol.* 188 (1), 163–169. <https://doi.org/10.4049/jimmunol.1101254>.
- Nakahama, K., 2010. Cellular communications in bone homeostasis and repair. *Cell. Mol. Life Sci.* 67 (23), 4001–4009. <https://doi.org/10.1007/s00018-010-0479-3>.
- Napoli, N., Chandran, M., Pierroz, D.D., Abrahamsen, B., Schwartz, A.V., Ferrari, S.L., 2017. Mechanisms of diabetes mellitus-induced bone fragility. *Nat. Rev. Endocrinol.* 13 (4), 208–219.
- Nie, Y., Li, S., Yi, Y., Su, W., Chai, X., Jia, D., Wang, Q., 2014. Effects of astragalus injection on the TGF β /Smad pathway in the kidney in type 2 diabetic mice. *BMC Compl. Alternative Med.* 14, 148. <https://doi.org/10.1186/1472-6882-14-148>.
- Portha, B., 2005. Programmed disorders of beta-cell development and function as one cause for type 2 diabetes? The GK rat paradigm. *Diabetes Metab Res Rev* 21 (6), 495–504. <https://doi.org/10.1002/dmrr.566>.
- Ralph D, L.S., Massaro, Joseph, 2008. *Wiley Encyclopedia of Clinical Trials*.
- Shan, P.F., Wu, X.P., Zhang, H., Cao, X.Z., Yuan, L.Q., Liao, E.Y., 2011. Age-related bone mineral density, osteoporosis rate and risk of vertebral fracture in mainland Chinese women with type 2 diabetes mellitus. *J. Endocrinol. Invest.* 34 (3), 190–196. <https://doi.org/10.1007/bf03347065>.
- Shanbhogue, V.V., Mitchell, D.M., Rosen, C.J., Bouxsein, M.L., 2016. Type 2 diabetes and the skeleton: new insights into sweet bones. *The Lancet Diabetes & Endocrinology* 4 (2), 159–173.
- Strotmeyer, E.S., Cauley, J.A., Schwartz, A.V., Nevitt, M.C., Resnick, H.E., Bauer, D.C., Newman, A.B., 2005. Nontraumatic fracture risk with diabetes mellitus and impaired fasting glucose in older white and black adults: the health, aging, and body composition study. *Arch. Intern. Med.* 165 (14), 1612–1617.
- Sugatani, T., Hruska, K.A., 2005. Akt1/Akt2 and mammalian target of rapamycin/Bim play critical roles in osteoclast differentiation and survival, respectively, whereas Akt is dispensable for cell survival in isolated osteoclast precursors. *J. Biol. Chem.* 280 (5), 3583–3589. <https://doi.org/10.1074/jbc.M410480200>.
- Sun, L., Di, Y.M., Lu, C., Guo, X., Tang, X., Zhang, A.L., Fan, G., 2020. Additional benefit of Chinese medicine formulae including *Dioscoreae rhizome* (Shanyao) for diabetes mellitus: current state of evidence. *Front. Endocrinol.* 11, 553288. <https://doi.org/10.3389/fendo.2020.553288>.

- Tian, S., Li, Y., Li, D., Xu, X., Wang, J., Zhang, Q., Hou, T., 2013. Modeling compound-target interaction network of traditional Chinese medicines for type II diabetes mellitus: insight for polypharmacology and drug design. *J. Chem. Inf. Model.* 53 (7), 1787–1803. <https://doi.org/10.1021/ci400146u>.
- Vestergaard, P., 2007. Discrepancies in bone mineral density and fracture risk in patients with type 1 and type 2 diabetes—a meta-analysis. *Osteoporos. Int. : a journal established as result of cooperation between the European Foundation for Osteoporosis and the National Osteoporosis Foundation of the USA* 18 (4), 427–444. <https://doi.org/10.1007/s00198-006-0253-4>.
- Walsh, M.C., Kim, N., Kadono, Y., Rho, J., Lee, S.Y., Lorenzo, J., Choi, Y., 2006. Osteoimmunology: interplay between the immune system and bone metabolism. *Annu. Rev. Immunol.* 24, 33–63. <https://doi.org/10.1146/annurev.immunol.24.021605.090646>.
- Williams, G.A., Callon, K.E., Watson, M., Costa, J.L., Ding, Y., Dickinson, M., Cornish, J., 2011. Skeletal phenotype of the leptin receptor-deficient db/db mouse. *J. Bone Miner. Res.* 26 (8), 1698–1709. <https://doi.org/10.1002/jbmr.367>.
- Wu, M., Chen, W., Lu, Y., Zhu, G., Hao, L., Li, Y.P., 2017. Gα13 negatively controls osteoclastogenesis through inhibition of the Akt-GSK3β-NFATc1 signalling pathway. *Nat. Commun.* 8, 13700. <https://doi.org/10.1038/ncomms13700>.
- Xiao, D., Zhou, Q., Gao, Y., Cao, B., Zhang, Q., Zeng, G., Zong, S., 2020. PDK1 is important lipid kinase for RANKL-induced osteoclast formation and function via the regulation of the Akt-GSK3β-NFATc1 signaling cascade. *J. Cell. Biochem.* 121 (11), 4542–4557. <https://doi.org/10.1002/jcb.29677>.
- Xiong, M.Q., Lin, A.Z., Zhu, Z.Z., 1997. [Effects of supplemented taohe chengqi decoction in treating insulin resistance in rats with non-insulin dependent diabetes mellitus]. *Zhongguo Zhong Xi Yi Jie He Za Zhi* 17 (3), 165–168.
- Xu, H.Y., Zhang, Y.Q., Liu, Z.M., Chen, T., Lv, C.Y., Tang, S.H., Huang, L.Q., 2019. ETCM: an encyclopaedia of traditional Chinese medicine. *Nucleic Acids Res.* 47 (D1), D976–d982. <https://doi.org/10.1093/nar/gky987>.
- Yang, L., Chen, J., Lu, H., Lai, J., He, Y., Liu, S., Guo, X., 2019. Pueraria lobata for diabetes mellitus: past, present and future. *Am. J. Chin. Med.* 47 (7), 1419–1444. <https://doi.org/10.1142/s0192415x19500733>.
- Yeu, J., Ko, H.J., Kim, D., Ahn, Y., Kim, J., Lee, W., Lee, S.J., 2019. Evaluation of iNSiGHT VET DXA (Dual-Energy X-ray Absorptiometry) for assessing body composition in obese rats fed with high fat diet: a follow-up study of diet induced obesity model for 8 weeks. *Lab Anim Res* 35, 2. <https://doi.org/10.1186/s42826-019-0004-2>.
- Yoon, J., Leiter, E., Coleman, D., Kim, M., Pak, C., McArthur, R., Roncari, D., 1988. Genetic control of organ-reactive autoantibody production in mice by obesity (ob) diabetes (db) genes. *Diabetes* 37 (9), 1287–1293. <https://doi.org/10.2337/diab.37.9.1287>.
- Yue, S.J., Liu, J., Feng, W.W., Zhang, F.L., Chen, J.X., Xin, L.T., Yan, D., 2017. System pharmacology-based dissection of the synergistic mechanism of Huangqi and huanglian for diabetes mellitus. *Front. Pharmacol.* 8, 694. <https://doi.org/10.3389/fphar.2017.00694>.
- Zhang, Y., Luo, J.X., Hu, X.Y., Yang, F., Zhong, S., Lin, W., 2016. Improved prescription of taohechengqi-tang alleviates D-galactosamine acute liver failure in rats. *World J. Gastroenterol.* 22 (8), 2558–2565. <https://doi.org/10.3748/wjg.v22.i8.2558>.
- Zhang, Y., Proenca, R., Maffei, M., Barone, M., Leopold, L., Friedman, J.M., 1994. Positional cloning of the mouse obese gene and its human homologue. *Nature* 372 (6505), 425–432. <https://doi.org/10.1038/372425a0>.
- Zhao, M.D., Li, J.Q., Chen, F.Y., Dong, W., Wen, L.J., Fei, W.D., Zheng, C.H., 2019. Co-delivery of curcumin and paclitaxel by "Core-Shell" targeting amphiphilic copolymer to reverse resistance in the treatment of ovarian cancer. *Int. J. Nanomed.* 14, 9453–9467. <https://doi.org/10.2147/ijn.S224579>.
- Zhou, S., Ai, Z., Li, W., You, P., Wu, C., Li, L., Ba, Y., 2020. Deciphering the pharmacological mechanisms of taohe-chengqi decoction extract against renal fibrosis through integrating network pharmacology and experimental validation in vitro and in vivo. *Front. Pharmacol.* 11, 425. <https://doi.org/10.3389/fphar.2020.00425>.
- Zhu, Z.Z., Xiong, M.Q., Lin, A.Z., 1997. [Effect of sanhuang jiangtang recipe on insulin peripheral resistance in type II diabetics]. *Zhongguo Zhong Xi Yi Jie He Za Zhi* 17 (10), 590–593.